



Research article

UDC 624.044.2

DOI: 10.34910/MCE.140.2



High-strength concrete behavior in post-limit conditions

P.D. Arleninov^{1,2} 

¹ JSC Research Center of Construction, Research Institute of Concrete and Reinforced Concrete (NII ZHB) named A.A. Gvozdev, Moscow, Russian Federation

² National Research Moscow State University of Civil Engineering, Moscow, Russian Federation

 arleninoff@gmail.com

Keywords: elastic modulus, limit state, descending branch, high-strength concrete, microcracks

Abstract. The objects of study were specimens of various shapes and aspect ratios made of high-strength modified concrete B90–B100 with a modified elastic modulus of 55,000 MPa. This modulus significantly exceeds the normative values specified in the building code SP 63.13330 when the concrete is loaded beyond its ultimate state. The need for this study stems from insufficient research on the deformation characteristics of high-strength concretes in extreme states (after reaching the ultimate load – with or without subsequent unloading), as well as the inapplicability of classical microcracking theories (Berg, Winter) to describe their behavior, which requires the development of new evaluation methods. Since high-strength concretes fail brittly, the research methods included two approaches to loading specimens – loading by stresses (standard method) and additionally by deformations up to the peak failure load with subsequent unloading and holding (from 1 hour to 8 days); the elastic modulus was determined according to GOST 24452 before and after loading, while microcrack development was monitored using ultrasonic testing methods (through-transmission and surface sounding). Based on the research results, it was established that during short-term holding (1 hour), the elastic modulus increased by 40–71 % (reaching 73,602–101,192 MPa) – this is explained by crack closure during specimen compression and the inertia of the stress relaxation process, while strength decreased by 20 %. After holding ≥ 1 day, the elastic modulus (49,684–57,683 MPa) and strength approached the initial values (± 6 %), despite visible damage to specimens after initial peak load attainment. At the same time, the ultrasonic wave travel time and Poisson's ratio (0.21–0.26) remained practically unchanged up to 90 % of the failure load, which does not correspond to classical microcracking development models. The main conclusions of the work: high-strength concretes retain nearly linear deformation behavior even after reaching the ultimate state. These results cast doubt on existing theoretical models describing crack formation processes and emphasize the importance of accounting for stress relaxation in structural assessments, as well as the necessity for comprehensive research on high-strength concretes.

Citation: Arleninov, P.D. High-strength concrete behavior in post-limit conditions. Magazine of Civil Engineering. 2025. 18(8). Article no. 14002. DOI: 10.34910/MCE.140.2

1. Introduction

This study investigated the behavior of modern high-strength heavy concrete under extreme conditions. The objects of research were prism specimens in accordance with GOST 24452-2023 currently in force in the territory of the Russian Federation with an aspect ratio of 1:4, and cylinder specimens with an aspect ratio of 1:2.

High-strength concretes are currently widely used in both civil and industrial construction, including in reinforced concrete [1, 3] and steel-reinforced concrete structures [4–5]. While the strength characteristics of high-strength concretes themselves and the influence of various factors on them have been studied to some extent, albeit insufficiently well, their deformation characteristics are significantly less

studied, as noted by many authors [6–8]; as for research on the extreme states of high-strength concrete behavior, such studies either do not exist at all or are isolated [9].

In which building structure operation scenarios is it necessary to know how concrete behaves in an extreme state? Several definitions of the extreme state of concrete behavior have been proposed by various authors [10–12]. First, let us define what we call an extreme state for this study. We will consider as extreme a state where a specimen is uniformly loaded to the maximum load it can withstand under a given loading method (the maximum load may differ under different loading methods), but is not brought to failure – unloading is performed, after which we study how such high stress levels in the specimen affected its main strength and deformation characteristics.

The relevance of the work lies in the fact that in certain scenarios, it is necessary to know the elastic modulus characteristics of non-uniform concrete already having internal structural defects – microcracks; and these are not necessarily structures operating at stress levels close to ultimate. In certain cases, microcracks can appear in a structural element during the concrete hardening stage – these can be shrinkage processes in reinforced concrete and especially steel-reinforced concrete structures, as well as thermal deformations during the hardening of concrete in massive structures accompanied by significant heat release and consequently the presence of a temperature gradient across the element's cross-section.

The use of a theoretical framework based on the fundamental research of Berg et al. [13], both in its original form (c 1) and based on modified theories [14–16], does not yield reliable results – Formulas (2), (3) respectively. Study [17] only processes previously obtained experimental data [18–20] without proposing its own expression for predicting microcracking processes.

release and consequently the presence of a temperature gradient across the element's cross-section.

The use of a theoretical framework based on the fundamental research of Berg et al. [13], both in its original form (c 1) and based on modified theories [14–16], does not yield reliable results – Formulas (2), (3) respectively. Study [17] only processes previously obtained experimental data [18–20] without proposing its own expression for predicting microcracking processes.

$$\frac{R_{crc}^0}{R_b} = 0.35 \cdot \lg R_b - 0.5, \quad \frac{R_{crc}^v}{R_b} = 0.35 \cdot \lg R_b - 0.175; \quad (1)$$

$$\frac{R_{crc}^0}{R_b} = 0.33 \cdot K_{crc} \ln R_b - 0.15, \quad \frac{R_{crc}^v}{R_b} = 0.35 \cdot \lg R_b + 0.1; \quad (2)$$

$$R_{crc}^0 = \left(1 - e^{-0.052 \cdot R_b^{0.642}}\right) \cdot R_b, \quad R_{crc}^v = 4.652 \cdot R_b^{0.642} \cdot R_{crc}^0, \quad (3)$$

where R_T^0 , R_T^v are the parametric points of the conditional lower and upper levels of cracking relative to the prismatic strength R_b ; K_{crc} – empirical coefficient equal to 1 for heavy concrete.

In this regard, the A.A. Gvozdev Research Institute of Concrete and Reinforced Concrete (NIIZhB) set the goal of conducting extensive experimental-theoretical studies aimed at developing a standardized methodology for experimentally determining crack formation limits in high-strength concretes, as well as options for physical modeling of microcracks with assessment of their influence on the strength and deformation characteristics of concrete specimens. In other words, sometimes it is necessary to understand how a structure or structural element will behave after being subjected to loads exceeding design resistance for some time and having potentially sustained damage in the form of microstructural failures.

As for normal-strength concretes, according to the classical theory of Berg (which, incidentally, does not contradict research by American specialists from Cornell University under the guidance of Professor Winter [18–20] conducted in the 1960–1970s – most subsequent theoretical studies are based on these experiments), microcracks in concrete begin to develop approximately after reaching 0.4–0.5 of the failure load (which to some extent corresponds to the level of design concrete resistance), and closer to stress levels of 0.7–0.8 of the failure load, the intensity of microdamages increases significantly. The different levels of microcrack formation according to Berg and Winter can be graphically represented in Figs. 1 and 2.

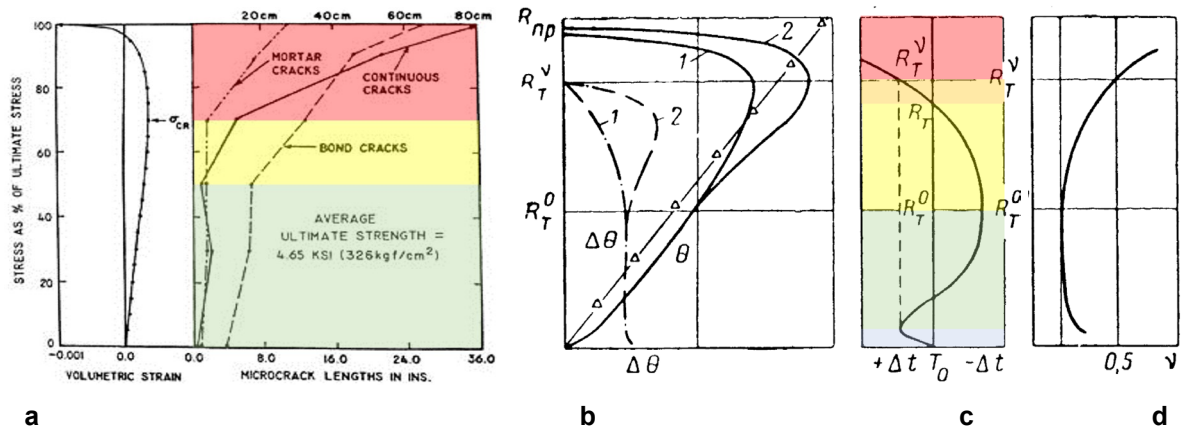


Figure 1. a) The dependence of the total length of microcracks on the stress level (Winter); b, c, d) the dependence of volumetric deformations, ultrasound transmission time, and Poisson's ratio on the stress level, respectively (Berg): grey – decompression of the least stable structures; green – compaction of the material; yellow – development of micro-fractures; orange – intensive development of micro-fractures; red – a sharp increase in the length of microcracks.

The research presented in this article is a part of the extensive work described above. The impact of micro-fractures of the concrete structure on the modulus of elasticity at stress levels close to the destructive load was evaluated.

2. Materials and Methods

2.1. Materials Employed

Experimental studies were conducted on high-strength self-sealing heavy concrete B90-B100 on standard materials used in the Russian Federation (Portland cement, sand, crushed stone, active mineral additives, complex additives). The initial modulus of elasticity of concrete was 55,000 MPa. This particular composition with a modified modulus of elasticity was chosen relative to the one given in SP 63.13330 (43,000 MPa), since concretes of classes higher than B80 are usually used in high-rise construction and there an increase in the modulus of elasticity is almost always critical and the use of concretes of such classes with a conventional modulus of elasticity is not entirely rational [21, 22]. Sika additives were used directly in this composition, but concrete with the same characteristics can also be obtained with analog additives.

2.2. Test Methodology

From the prepared mixtures, specimens were molded: cubes with dimensions 100×100×100 mm, 150×150×150 mm for determining cube compressive strength according to GOST 10180 and GOST 31914; prisms 100×100×400 mm, prisms 150×150×600 mm, and cylinders Ø150×600 mm. Fig. 2 shows the types of tested specimens (the research discussed in this article was conducted only on the specified specimens, but in a larger comprehensive study, specimens with greater variability of geometric dimensions were tested – in addition to the above-mentioned prisms and cylinders, studies were performed on cylinders of all diameters 70, 100, and 150 mm, as well as on specimens with various cross-section to height ratios from 1:2 to 1:4). The measurement base included tensometry, dial indicators, portable deformometer, ultrasonic devices of surface and through action. Mechanical and digital dial indicators were used when determining the modulus of elasticity in accordance with GOST 24452, at 70 % of the destructive load they were removed and measurements were performed using tensometry and removable deformometers based on the Demec principle.



Figure 2. Description of the test mode for determining the modulus of elasticity after operation in an extreme state in the axes stress level – test time.

Testing was conducted on 5 reference specimens (of each standard size), on which the modulus of elasticity and destructive load (R1) were determined in accordance with GOST 24452, 5 specimens that were loaded with deformations and used to obtain the descending branch and determine the peak load value sustained by the specimen (R2) – typically this load is somewhat less than that obtained in standard testing according to GOST 24452, and 4 specimens of various standard sizes, which were first loaded with deformations up to the peak value of destructive load, then unloaded, held for a certain time, and subsequently tested for modulus of elasticity and then to failure (R3). The obtained results were compared with the values of modulus of elasticity obtained on these same specimens at the beginning of the experiment. The general testing scheme is shown in Fig. 3.

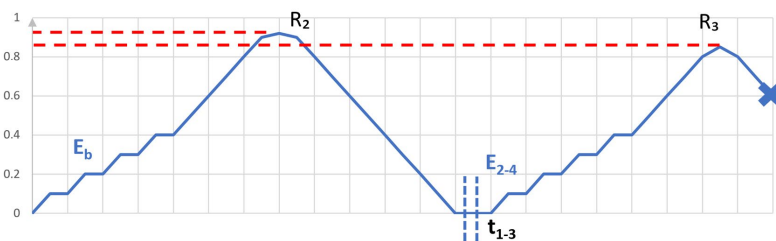


Figure 3. Description of the test mode for determining the modulus of elasticity after operation in an extreme state in the axes stress level – test time.

Loading by deformations was performed because high-strength concretes behave elastically almost up to failure, which occurs instantaneously and is accompanied by a sharp crack – essentially an explosion. Determining the peak load without specimen failure and consequently obtaining the descending branch in the $\sigma - \varepsilon$ graph is a rather complex task, and solving it by trivial methods is far from always possible [23, 24].

The determination of the microcrack initiation level in concrete was carried out according to the classical method of Professor Berg (Fig. 1b, c, d). For this purpose, at each loading stage, the specimens in the press were subjected to ultrasonic testing using ultrasonic testing devices. Both surface and through sounding were performed (see Fig. 4a) using UK-1401 and Pulsar 1.0 devices, respectively. During through sounding, a wet contact was used, so to ensure experimental purity, the device was rigidly fixed to the specimen, not removed, and measurements were taken in one section at the center of the specimen.

For surface sounding, 12 control points were marked on the lateral surface for conducting 6 measurements (using the UK-1401 device) – 3 vertically and 3 diagonally at angles from 45 to 70° to the horizontal. Fig. 4b shows a specimen brought to peak destructive load (immediately unloaded after reaching it) for subsequent elastic modulus testing. As can be seen from the figure, the specimen retained its shape but sustained several damages (chips and cracks) visible to the naked eye. On different specimens, these damages varied in appearance but were mostly concentrated at the edges, although some specimens exhibited vertically oriented cracks extending almost the full height of the specimen.

Fig. 3 indicates various holding intervals for the specimens to allow stress relaxation to occur. According to the results presented in the following section, the significant influence of stress relaxation is evident. The destructive load R3 also differs from loads R1 and R2, as shown below.

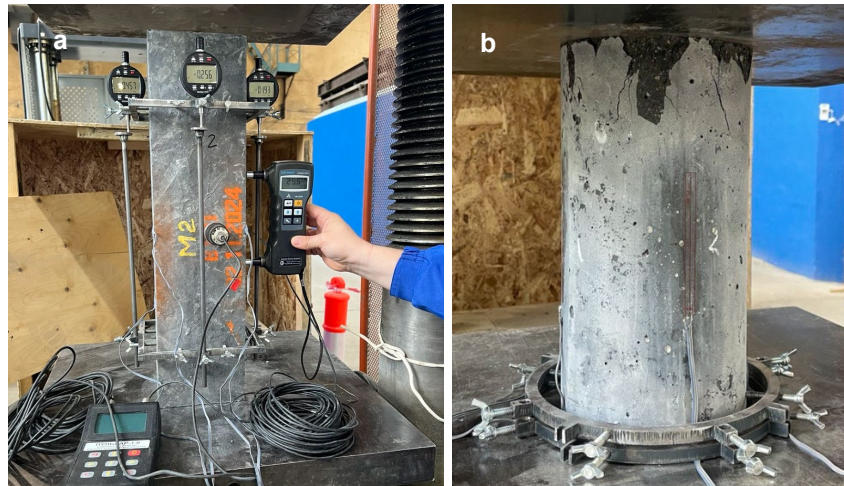


Figure 4. a) A cylinder sample brought to a destructive load during testing, but not destroyed; b) Ultrasonic sounding systems for the sample.

3. Results and Discussion

During the testing, ultrasonic monitoring could be conducted right up to specimen failure (up to 0.98–0.99 of the destructive load). However, through-transmission testing using the specified equipment yielded no results – the ultrasonic wave transit time remained virtually unchanged until specimen failure, possibly due to the orientation of microcracks in the specimen.

The pattern of changes in the ultrasonic transit time graph during measurements from one side up to stress levels of 0.6 of the destructive load closely resembles classical research (referring only to the qualitative behavior of the curve). Beyond the 0.6 stress level, the curve does not change direction, and up to loads approaching 0.9 of the destructive load, the ultrasonic wave transit time remains unchanged (see Fig. 5b).

Even at stress levels from 0.9 up to failure, there was no sharp decrease in ultrasonic transit time that would indicate a rapid increase in micro-failure volume. All this suggests qualitatively different behavior of high-strength concrete under loads entering the nonlinear region.

In Fig. 5a, using one of the specimens as an example, the development of volumetric deformations under load is shown – here the differences from classical theories are even more pronounced, as the curve never reached a plateau. The Poisson's ratio was recorded to vary from 0.21 to 0.26 (the graph of Poisson's ratio variation versus stress level is shown in Fig. 5c).

As previously mentioned, attempts to use formulas from both Berg's classical theory [13] and modified versions [14–15] for predicting microcrack development processes in concrete failed to yield positive results. Below are the results of determining microcrack formation boundaries using Formulas (1) and (2); other tested expressions showed even greater discrepancies with experimental results.

$$\text{According to Formula (1): } \frac{R_{crc}^0}{R_b} = 0.537; \frac{R_{crc}^v}{R_b} = 0.862.$$

$$\text{According to Formula (2): } \frac{R_{crc}^0}{R_b} = 0.857; \frac{R_{crc}^v}{R_b} = 1.107.$$

Berg's formula, as can be seen, gives too low values for the parametric points R_{crc}^0 and R_{crc}^v , although the proposed theory's description indicates its applicability to high-strength concretes with strength classes up to 100 MPa. Formula (2) shows a lower microcrack formation boundary much closer to the experimental results, but when determining the upper boundary, a mathematical error occurs (value greater than 1).

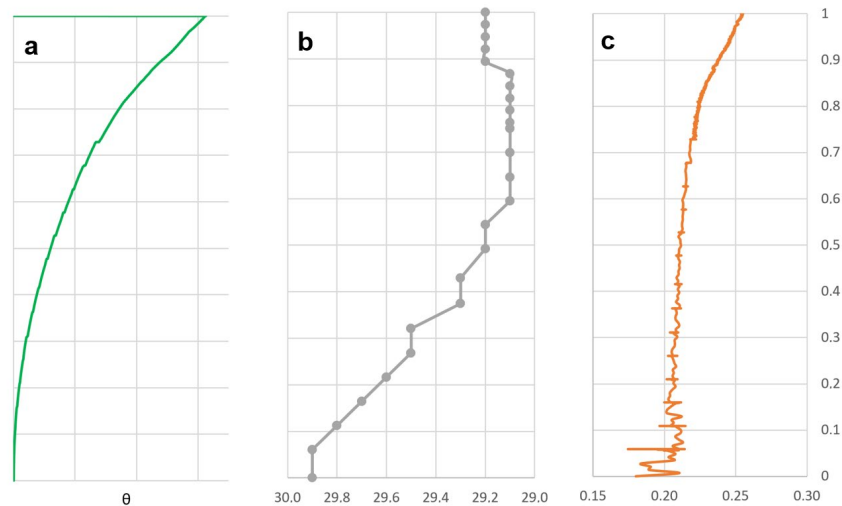


Figure 5. a) The dependence of volumetric deformations on the stress level; b) the dependence of the transit time on the stress level; c) the dependence of the Poisson's ratio on the stress level.

According to the test results, the following values of the modulus of elasticity were recorded after the concrete reached its ultimate load and various holding periods after unloading before reloading, compared with the initial modulus of elasticity determined directly on the same specimen.

$E_b = 53,000 \text{ MPa}$ – average initial modulus of elasticity for the group of specimens.

$E_{b1} = 59,141 \text{ MPa}$, $E_1 = 1.71 E_b$ (101,192 MPa) – modulus of elasticity determined almost immediately after reaching the failure load followed by unloading (stress relaxation holding period was about 1 hour). Specimen: cylinder $\varnothing 150 \times 300 \text{ mm}$.

$E_{b2} = 52,335 \text{ MPa}$, $E_2 = 1.41 E_b$ (73,602 MPa) – modulus of elasticity determined almost immediately after reaching the failure load followed by unloading (stress relaxation holding period was about 1 hour). Specimen: cylinder $\varnothing 150 \times 300 \text{ mm}$.

$E_{b3} = 54,314 \text{ MPa}$, $E_3 = 1.06 E_b$ (57,683 MPa) – modulus of elasticity determined on an unloaded specimen after a free-state holding period of 8 days. Specimen: cylinder $\varnothing 150 \times 300 \text{ mm}$.

$E_{b4} = 57,778 \text{ MPa}$, $E_4 = 1.00 E_b$ (57,967 MPa) – modulus of elasticity determined on an unloaded specimen after a free-state holding period of 3 days. Specimen: prism $150 \times 150 \times 600 \text{ mm}$.

$E_{b5} = 52,042 \text{ MPa}$, $E_5 = 1.00 E_b$ (51,994 MPa) – modulus of elasticity determined on an unloaded specimen after a free-state holding period of 1 day. Specimen: prism $150 \times 150 \times 600 \text{ mm}$.

Analysis of these results shows that with short holding periods after reaching the failure load, despite accumulated damage, the concrete's modulus of elasticity significantly increased by 1.4 to 1.7 times. This may be related to the deformation mechanics of high-strength concrete under extreme loads – nearly linear deformation until failure, minimal accumulation of internal defects (microcracks) and their closure at even higher stress levels, and certain inertia in the relaxation process of internal stresses after removing compressive load. These results are new and previously unpublished.

With holding periods of one day or more, significant relaxation of internal stresses occurs in the specimen, and the obtained modulus of elasticity values become close to the initial modulus ($\pm 6 \%$). Such results are also extremely unusual since the already failed specimen retained its basic initial deformation characteristics.

A crucial aspect in this case is the duration of the holding period sufficient for the residual post-unloading stresses to relax. Its exact value depends on many factors, primarily the concrete mix composition; thus, it may differ for each concrete type. In this experiment, several scenarios of post-loading holding periods were considered, and one day can be taken as an averaged, sufficient period for the relaxation of all internal stresses.

If we compare the already destructive loads, in particular R1, R2, R3, the generally expected results were recorded in qualitative perception, but the quantitative figures are somewhat unusual:

R1 = 88.2–99.5 MPa is the average destructive load during testing according to GOST 24452, depending on the type of sample;

R21 = 92.3 MPa, R31 = 72.7 MPa – cylinder $\varnothing 150 \times 300 \text{ mm}$; exposure time is 1 hour;

R22 = 92.5 MPa, R32 = 80.6 MPa – cylinder Ø150×300 mm; exposure time is 1 hour;

R23 = 96.4 MPa, R33 = 94.7 MPa – cylinder Ø150×300 mm; exposure for 8 days;

R24 = 85.3 MPa, R34 = 83.3 MPa – prism 150×150×600 mm; exposure for 1 day;

R25 = 89.0 MPa, R35 = 87.0 MPa – prism 150×150×600 mm; exposure for 3 days.

Analyzing these results, it can be seen that all tested samples show a decrease in load R2 relative to load R1 by 6 %, and load R3 relative to load R2 by 20 % for short exposures of an hour, and only 2 % for exposures of more than a day. To summarize, with short exposures, there was a significant increase in the modulus of elasticity but at the same time a significant decrease in the strength of concrete. At exposures of more than a day, all data stabilized, approaching the initial results. These results are of great interest and confirm one of the most important roles of the stress relaxation process in concrete. Research needs to be continued on different types under different test scenarios.

4. Conclusions

A series of experimental studies were conducted to determine the main deformation characteristics of high-strength concretes after their operation in the post-peak state, where creating such conditions for concrete itself represents a separate complex engineering task that was incidentally solved during this work. The research was performed on concrete specimens with compressive strength class B90-B100 and modified modulus of elasticity of 55,000 MPa. Based on the results of this work, several important conclusions can be drawn. Firstly, it allows for an assessment of the applicability of established approaches used to describe the deformation process of concretes.

- Classical theories for determining the level of microcrack formation and their derivatives describing the behavior of high-strength concretes are not fully applicable to high-strength concretes (more detailed studies on microcrack appearance in high-strength concretes will be presented in a separate article).
- Secondly, new results were obtained for the investigated mix composition, which can, however, be extrapolated to other modern modified high-strength concretes:
- High-strength concretes can demonstrate nearly linear behavior not only up to high stress levels close to failure but also after reaching their failure load (exceeding the limit state).
- No significant reduction was observed in the modulus of elasticity measured on unloaded specimens after they reached their limit state.
- The duration of concrete specimen holding after reaching their ultimate failure load significantly affects the modulus of elasticity determined on unloaded specimens. Moreover, with short holding times, a sharp increase in the modulus of elasticity was recorded.
- These results are of great interest and confirm one of the most important roles of the stress relaxation process in concrete. Research needs to be continued on different types under different test scenarios.

References

1. Kapriellov, S.S., Sheinfeld, A.V., Al-Omais, D., Zaitsev, A.S. High-Strength Concretes in Constructions of Foundations of the High-Rise Complex "OKO" in MIBC "MOSCOW-CITY." *Industrial and Civil Construction*. 2017. 3. Pp. 53–57.
2. Kapriellov, S.S., Sheinfeld, A.V., Kardumyan, G.S., Chilin, I.A. About selection of compositions of high-quality concretes with organic-mineral modifiers. *Construction Materials*. 2017. 12. Pp. 58–63.
3. Polskoy, P.P., Mailyan, D., Beskopylny, A.N., Meskhi, B., Shilov, A.V., Umarov, A. Strength of Compressed Reinforced Concrete Elements Reinforced with CFRP at Different Load Application Eccentricity. *Polymers*. 2023. 15. Pp. 26. DOI: 10.3390/polym15010026
4. Lu, T., Jin, H., Guan, K. Experimental Research on Axial Compression Performance of High-Performance-Fiber-Reinforced-Cement-Composite-Prefabricated Monolithic Composite Columns. *Buildings*. 2023. 13. Pp. 1748–1763. DOI: 10.3390/buildings13071748
5. Ince, E.G., Özkal, F.M. Optimization of Structural Steel Used in Concrete-Encased Steel Composite Columns via Topology Optimization. *Applied Sciences*. 2024. 14(3). Article no. 1170. DOI: 10.3390/app14031170
6. Bezgodov, I., Kapriellov, S., Sheynfeld, A. Relationship between Strength and Deformation Characteristics of High-Strength Self-Compacting Concrete. *International Journal for Computational Civil and Structural Engineering*. 2022. 18(2). Pp. 175–183. DOI: 10.22337/2587-9618-2022-18-2-175-183
7. Domarova, E.V. Influence of Creep on the Stress-Strain State of Reinforced Concrete Multistory Buildings. *Construction and Reconstruction*. 2022. 3(101). Pp. 14–22. DOI: 10.33979/2073-7416-2022-101-3-14-22
8. Bezgodov, I.M., Kapustin, D.E., Efishov, L.I. Physical-Mechanical and Rheological Characteristics of High-Strength Concrete and Granite. *Industrial and Civil Construction*. 2024. 8. Pp. 48–56. DOI: 10.33622/0869-7019.2024.08.48-56
9. Kolchunov, V.I., Ilyushchenko, T.A. Kriterii osobogo predelnogo sostoyaniya ramnykh sistem iz vysokoprochnogo zhelezobetona [Criteria for special limit states of frame systems made of high-strength reinforced concrete]. *Bezopasnost stroitel'nogo fonda*

- Rossii. problemy i resheniya [Safety of Russia's Building Stock. Problems and Solutions: Proceedings of International Academic Readings]. Kursk: Universitetskaya kniga, 2023. Pp. 64–72.
10. Bondarenko, V.M., Kljueva, N.V., Kolchunov, V.I., Androsova, N.B. Some Results of Analysis and Scientific Research on Structural Safety and Survivability Theory. Construction and Reconstruction. 2012. 4(42). Pp. 3–16.
 11. Kolchunov, V., Fedorov, S. Serviceability Limit State Parameters for High Strength Concrete Structures. International Journal for Computational Civil and Structural Engineering. 2024. 20(3). Pp. 145–158. DOI: 10.22337/2587-9618-2024-20-3-145-158
 12. Wang, T., Zhang, L., Zhao, H., Chen, Q. Progressive collapse resistance of reinforced-concrete frames with specially shaped columns under loss of a corner column. Magazine of Concrete Research. 2016. 68(9). Pp. 435–449. DOI: 10.1680/jmacr.15.00108
 13. Berg, O.Ya., Shcherbakov, E.N., Pisanko, G.N. Vysokoprochnyy beton [High-strength concrete]. Moscow: Stroyizdat, 1971. 209 p.
 14. Istomin, A.D., Belikov, N.A. Dependence of the Borders of the Microcreeping in Concrete from Strenqs and Strain Condition. Bulletin of MGSU. 2011. 2-1. Pp. 159–162.
 15. Semenyuk, S.D., Moskalkova, Yu.G. Methods for determining the limits of the microcrack formation. Construction of Unique Buildings and Structures. 2018. 7(70). Pp. 22–30.
 16. Zinoviev, V.N. Opredeleniye mikrotreshchinoobrazovaniya betona pri szhatii tenzometricheskim metodom [Determination of concrete microcracking under compression by strain gauge method]. Izvestiya KGTU. 2010. 17. Pp. 118–122. (rus)
 17. Tyukalov, Yu.Ya. Rectangular flat finite element for modeling the process of crack formation. Magazine of Civil Engineering. 2025. 18(3). Article no. 13502. DOI: 10.34910/MCE.135.2
 18. Hsu, T.T.C., Slate, F.O., Sturman, G.M., Winter, G. Microcracking of Plain Concrete and the Shape of Stress-Strain Curve. JACI. 1963. 60(2). Pp. 209–223. DOI: 10.14359/7852
 19. Slate, F.O., Olsefski, S. X-Rays for Study of Internal Structure and Microcracking of Concrete. 1963. JACI Proceedings. 60(5). Pp. 575–587.
 20. Shah, S.P., Chandra, S. Critical Stress, Volume Change, and Microcracking of Concrete. JACI Proceedings. 1968. 65(9). Pp. 770–778.
 21. Kapriyelov, S.S., Sheinfeld, A.V., Selyutin, N.M. Control of Heavy Concrete Characteristics Affecting Structural Stiffness. International Journal for Computational Civil and Structural Engineering. 2022. 18(1). Pp. 24–39. DOI: 10.22337/2587-9618-2022-18-1-24-39
 22. Kolchunov, V., Fedorov, S. Serviceability Limit State Parameters for High Strength Concrete Structures. International Journal for Computational Civil and Structural Engineering. 2024. 20(3). Pp. 145–158. DOI: 10.22337/2587-9618-2024-20-3-145-158
 23. Bezgodov, I.M. Methodological Features of the Study of Complete Diagrams of Deformation and Stress Relaxation in Concrete. Concrete Technologies. 2020. 11–12(172–173). Pp. 39–44.
 24. Eryshev, V.A., Karpenko, N.I., Zhemchuyev, A.O. Integral Parameters of Concrete Diagrams for Calculations of Strength of Reinforced Concrete Elements Using the Deformation Model. International Journal for Computational Civil and Structural Engineering. 2020. 16(1). Pp. 25–37. DOI: 10.22337/2587-9618-2020-16-1-25-37

Information about the authors:

Petr Arlenin, PhD in Technical Sciences

E-mail: arleninoff@gmail.com

Received 07.08.2025. Approved after reviewing 16.11.2025. Accepted 17.11.2025.